Electrodeposited nano-porous and neural network-like Ln@HOF film for SO_2 gas quantitative detection via fluorescent sensing and machine learning

Xin Xu,[a] Wanpeng Ma,[a] and Bing Yan*,[a]

[a] *Shanghai Key Lab of Chemical Assessment and Sustainability, School of Chemical Science and Engineering, Tongji University, Siping Road 1239, Shanghai 200092, China. E-mail: byan@tongji.edu.cn.*

Electronic supplementary information

Materials and physical measurements

Fig. S1. (a) XPS spectra of Tb 4d electron in Tb@ME-IPA. (b-d) XPS spectra of N 1s electron in ME-IPA, Tb@ME-IPA and **1**. (e-g) XPS spectra of O 1s electron in $Tb(NO_3)_3{\cdot}6H_2O$, Tb@ME-IPA and **1**.

Fig. S2. Picture of **1** viewed from different angles.

Fig. S3. (a-d) SEM pictures of **1**.

Fig. S4. (a) SEM image of **1**. (b–e) EDX mapping images of C, N, O and Tb elements in **1**. (f) The element content of C (53.52%), N (36.52%), O (8,39%), Tb (1.57%) elements in EDX energy spectrum of **1**.

Fig. S5. (a) Emission spectrum of ME-IPA upon λ_{ex} = 310 nm. (b) Excitation spectrum of **1** by monitoring the 545 nm emission peak. (c) Schematic diagram for TADF-assisted ET and LMCT-induced ET progresses for **1** (ISC: intersystem crossing; RISC: reverse intersystem crossing; TADF: thermally activated delayed fluorescence).

Fig. S6. (a-b) Dependence of emission intensity for **1** on temperature (30–60 °C) upon λ_{ex} = 290 nm.

Fig. S7. Emission spectra of **1** taken out from different gas atmospheres with a concentration of 10^{-2} mol/L (λ_{ex} = 290 nm).

Fig. S8. (a) Emission spectra of **1** and 1-SO_2 (λ_{ex} = 290 nm). (b) CIE diagram for indicating the emitting color transfer of **1** from (0.2103, 0.7623) to (0.1673, 0.0452) (λ_{ex} = 290 nm).

Fig. S9. (a) Response time of **1** toward SO_2. (b) Luminescence intensity of 545 nm peak for **1** after seven repetitions in recycling experiment of SO_2 sensing.

Fig. S10. (a) SEM image of 1-SO_2. (b–f) EDX mapping images of C, N, O and Tb elements in 1-SO_2. (g) The element content of C (45.71%), N (35.97%), O (16.36%), S (0.32%) and Tb (1.64%) elements in EDX energy spectrum of 1-SO_2.

Fig. S11. (a) Emission spectrum of 1-SO_2 (C_{SO2} = 10^{-2} M). (b) Decay lifetime of 545 nm emission peak of **1** (λ_{ex} = 290 nm). (c) Emission spectra of ME and IPA powders. (d) PXRD patterns of **1** and 1-SO_2.

Fig. S12. (a) Emission spectra of Tb@ME-IPA in various anion solution (C = 10^{-2} M) (λ_{ex} = 290 nm). (b) Emission intensity of 545nm peak in various anion solution (C = 10^{-2} M). (c) Emission spectra of Tb@ME-IPA and Tb@ME-IPA-SO_3^{2-} (C = 10^{-2} M) (λ_{ex} = 290 nm). (d) Decay lifetimes of 545 nm emission peak for Tb@ME-IPA and Tb@ME-IPA-SO_3^{2-} (C = 10^{-2} M) (λ_{ex} = 290 nm).

Fig. S13. (a) Emission spectra of Tb@ME-IPA in various SO_3^{2-} solutions with a successive concentration (C = 10^{-8}-10^{-2} M) (λ_{ex} = 290 nm). (b) Dependence of emission intensity of 545 and 380 nm peaks on SO_3^{2-} concentration. (c) Emitting pictures of Tb@ME-IPA in various SO_3^{2-} solutions with a successive

concentration (C = 10^{-8}-10^{-2} M) (λ_{ex} = 290 nm). (d) Dependence of emission intensity ratio of 380 and 545 nm peaks on SO_3^{2-} concentration (C = 10^{-8}-10^{-2} M) (e) Calibration curves of Tb@ME-IPA toward SO_3^{2-} in the concentration range of 10^{-8}-10^{-2} M. (f) Response time of Tb@ME-IPA toward SO_3^{2-}.

Fig. S14. (a) Emission spectra of Tb@ME-IPA in various serum components (C = 10^{-2} M) (λ_{ex} = 290 nm). (b) Histogram of 545 nm emission peak of Tb@ME-IPA in various serum components (C = 10^{-2} M). (c) Emission spectra of Tb@ME-IPA in serum system in various SO_3^{2-} solutions with a successive concentration (C = 10^{-8}-10^{-2} M) (λ_{ex} = 290 nm). (d) Dependence of emission intensity of 545 and 380 nm peaks on SO_3^{2-} concentration. (e) Dependence of emission intensity ratio of 380 and 545 nm peaks on SO_3^{2-} concentration (10^{-7}–10^{-2} M). (f) Calibration curves of Tb@ME-IPA toward SO_3^{2-} in the concentration range of 10^{-7}–10^{-2} M.

Fig. S15. Network training curve of the BPNN.

Fig. S16. Deviation curve of the BPNN (OV: original value; CV: calculated value).

Table S1. The reaction equations for preparation of various gases.

Table S2. Element contents of C, N, O, Tb in EDX energy spectrum **1** and C, N, O, S, Tb in EDX energy spectrum 1-SO_2.

Table S3. Summary of decay lifetime of **1**, 1-SO_2, Tb@ME-IPA, and Tb@ME-IPA-SO_3^{2-}.

Table S4. Summary of emission transitions and experimental energy gaps of ME-IPA and Tb^{3+} ions.

Table S5. Summary of R.G.B. of emitting color of **1** exposed in various SO_2 concentration (10^{-6}-10^{-2} M).

Table S6. Summary of input and output information during the training of BPNN for SO_2 detection.

Table S7. Network structure information.

Table S8. The summary of mean square error (MSE), original value (OV), calculated value (CV), variance (Var.)

Table S9. The summary of input and output information in real batch calculation during the test of BPNN.

Table S10. The matlab code of this BPNN.

Materials and physical measurements

All regents were used without further purification. Powder X-ray diffraction (PXRD) patterns were collected with a Bruker D8 ADVANCE diffractometer using Cu *Kα* radiation at 40 mA and 40 kV. SEM was performed on a Hitachi S-4800 field emission scanning electron microscope operating at 3 kV. Energy dispersive X-ray spectroscopy (EDX) and the EDX mapping image were obtained by the scanning electron microscope operating at 15 kV. X-ray photoelectron (XPS) spectra were recorded under ultrahigh vacuum ($<10^{-6}$ Pa) at a pass energy of 93.90 eV with an Axis Ultra DLD spectrometer (Kratos) by using a Mg K*α* (1253.6 eV) anode. All binding energies were adjusted by using contaminant carbon (C 1s = 284.8 eV). Fourier transform infrared (FT-IR) spectra were recorded using a Nicolet IS10 infrared spectrophotometer. The photoluminescence (PL) spectra, kinetics scan curve and phosphorescence decay lifetime curve were recorded on an Edinburgh FLS920 spectrophotometer with a 450 W xenon lamp as an excitation source.

The HOMO–LUMO energy levels were calculated by the DFT method at the b3lyp/6-31g level in the Gaussian 09W program package.

The BPNN model was constructed in Maishi Neural Network program package.

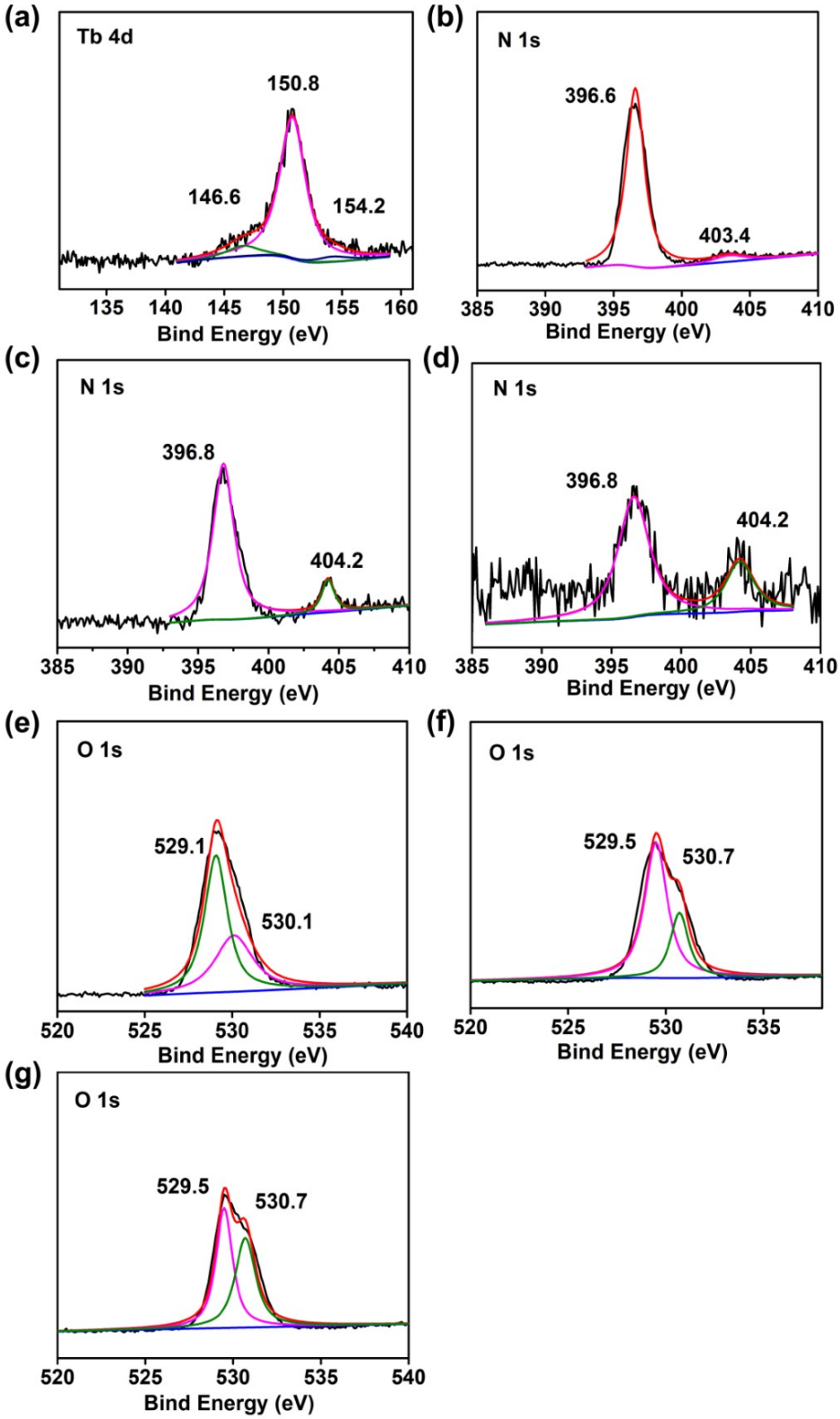

Fig. S1. (a) XPS spectra of Tb 4d electron in Tb@ME-IPA. (b-d) XPS spectra of N 1s electron in ME-IPA, Tb@ME-IPA and **1**. (e-g) XPS spectra of O 1s electron in $Tb(NO_3)_3 \cdot 6H_2O$, Tb@ME-IPA and **1**.

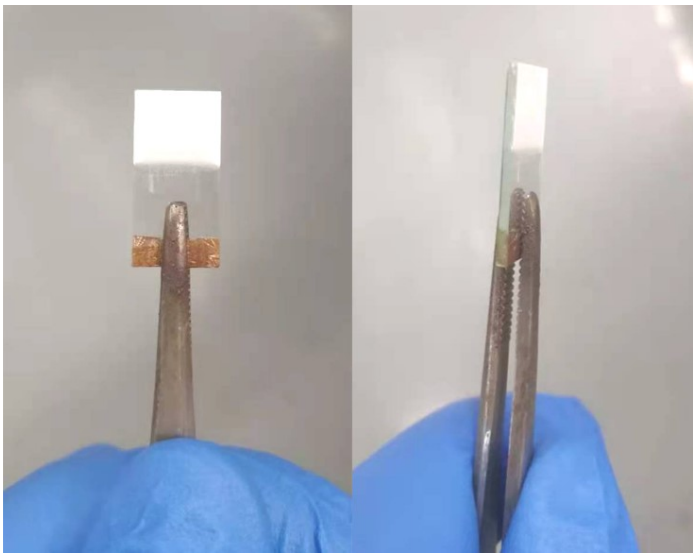

Fig. S2. Picture of **1** viewed from different angles.

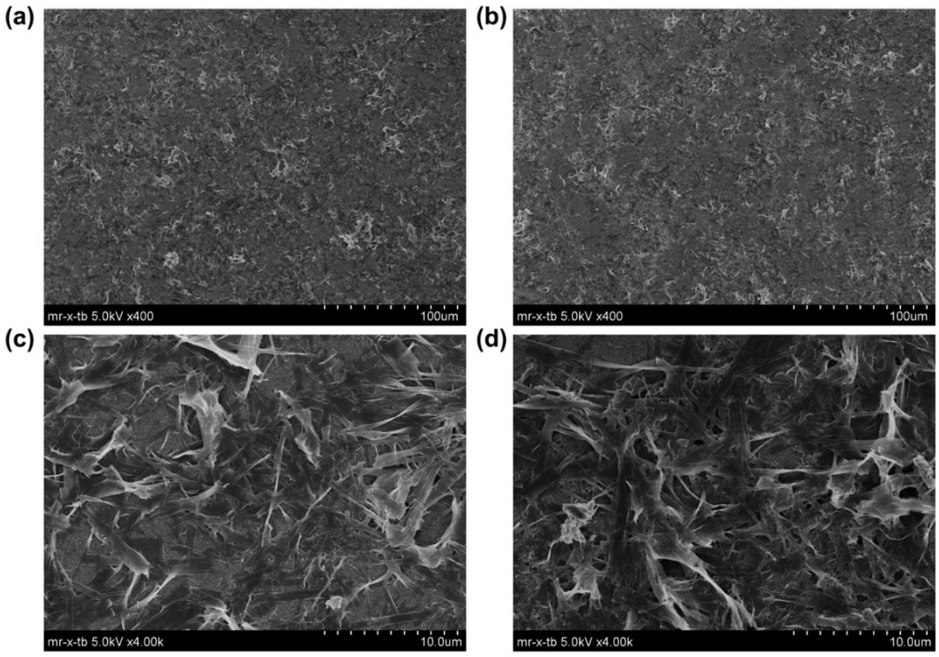

Fig. S3. (a-d) SEM pictures of **1**.

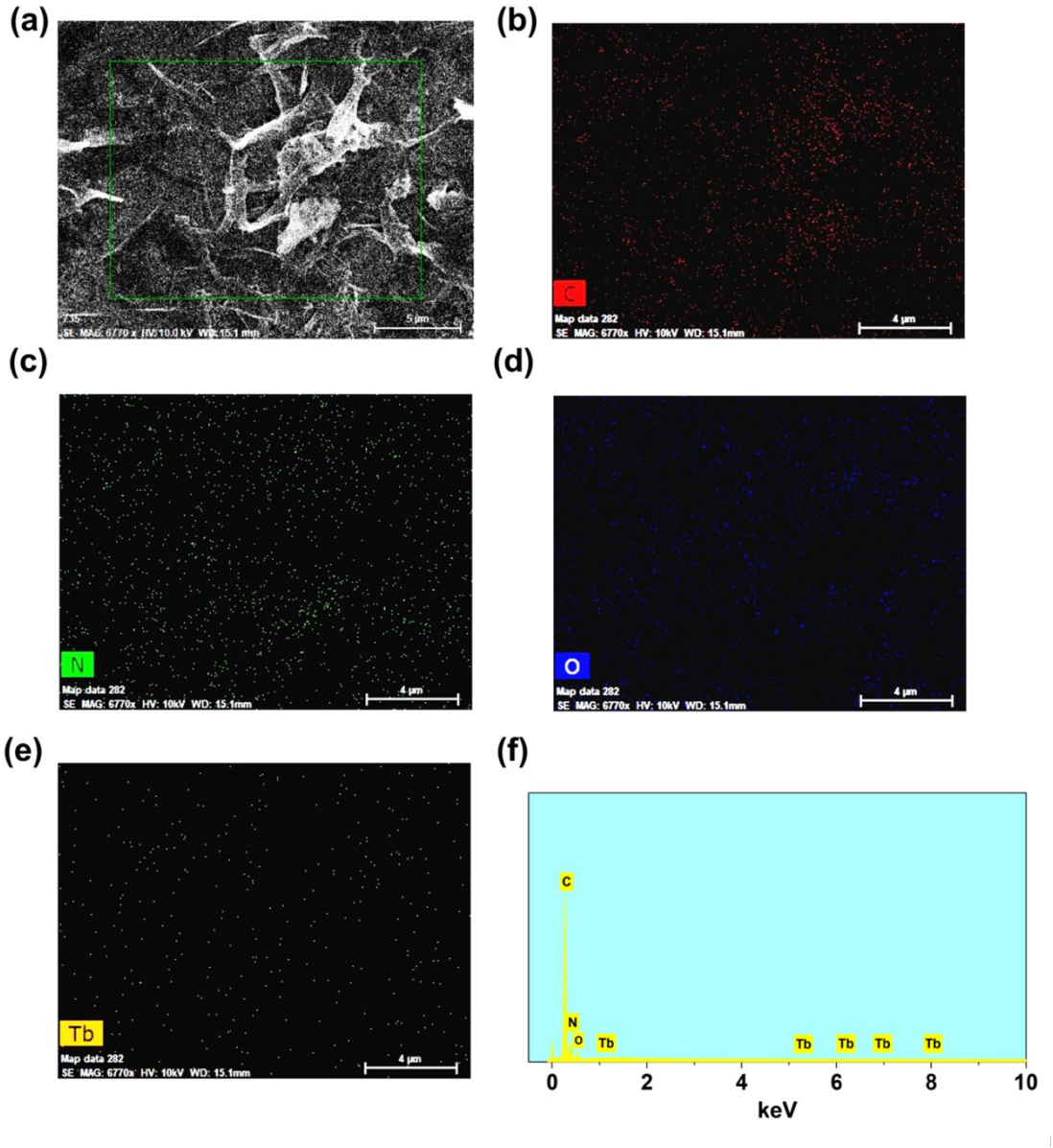

Fig. S4. (a) SEM image of **1**. (b–e) EDX mapping images of C, N, O and Tb elements in **1**. (f) The element content of C (53.52%), N (36.52%), O (8,39%), Tb (1.57%) elements in EDX energy spectrum of **1**.

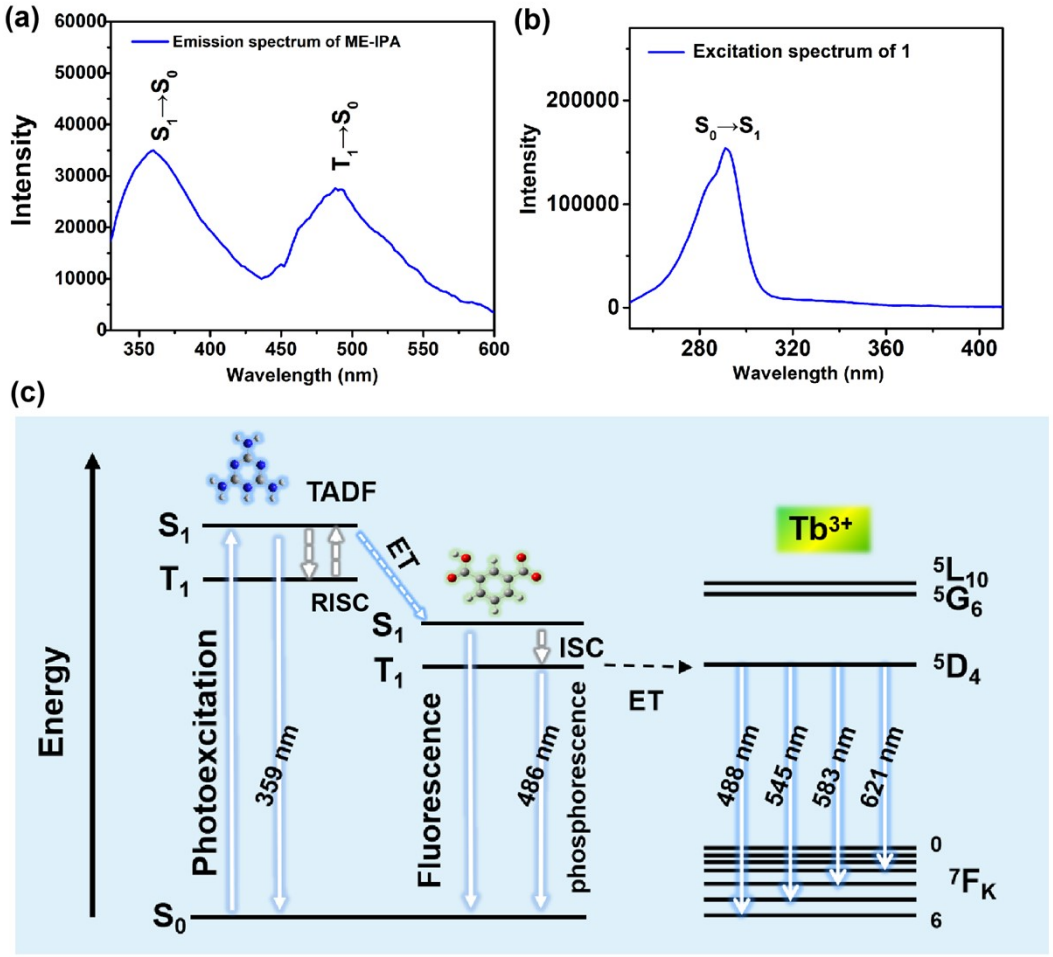

Fig. S5. (a) Emission spectrum of ME-IPA upon λ_{ex} = 310 nm. (b) Excitation spectrum of **1** by monitoring the 545 nm emission peak. (c) Schematic diagram for TADF-assisted ET and LMCT-induced ET progresses for **1** (ISC: intersystem crossing; RISC: reverse intersystem crossing; TADF: thermally activated delayed fluorescence).

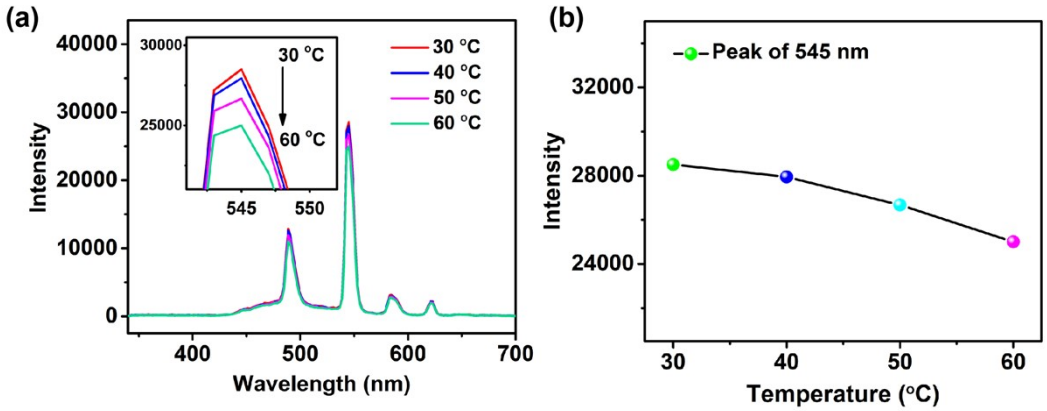

Fig. S6. (a-b) Dependence of emission intensity for **1** on temperature (30–60 °C) upon λ_{ex} = 290 nm.

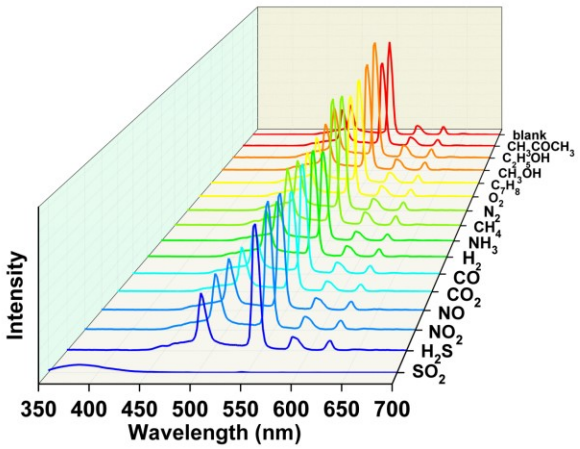

Fig. S7. Emission spectra of **1** taken out from different gas atmospheres with a concentration of 10^{-2} mol/L (λ_{ex} = 290 nm).

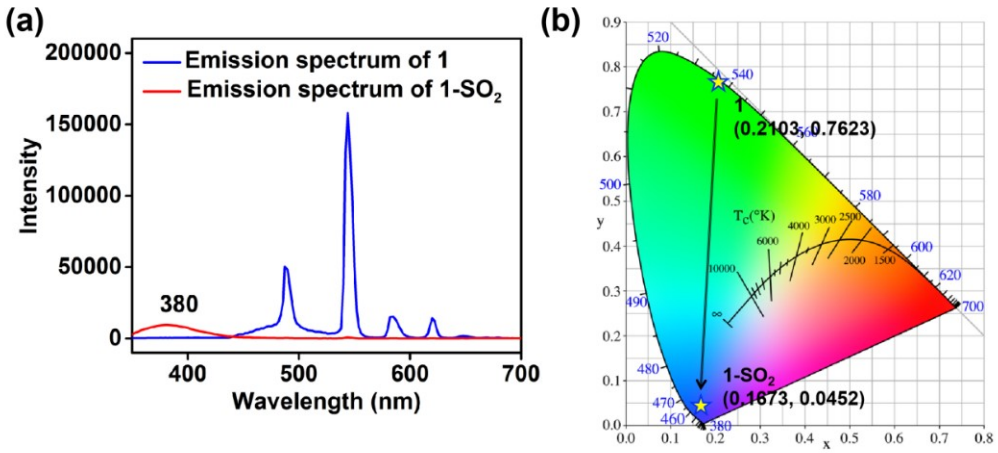

Fig. S8. (a) Emission spectra of **1** and 1-SO_2 (λ_{ex} = 290 nm). (b) CIE diagram for indicating the emitting color transfer of **1** from (0.2103, 0.7623) to (0.1673, 0.0452) (λ_{ex} = 290 nm).

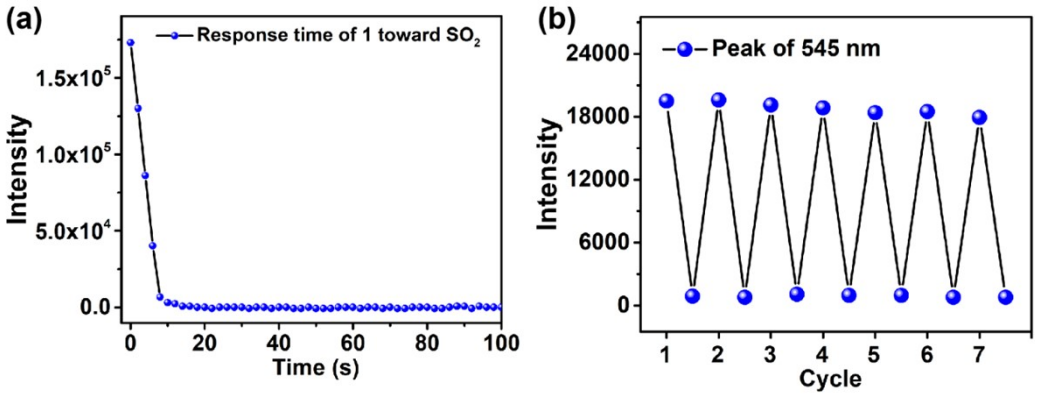

Fig. S9. (a) Response time of **1** toward SO_2. (b) Luminescence intensity of 545 nm peak for **1** after seven repetitions in recycling experiment of SO_2 sensing.

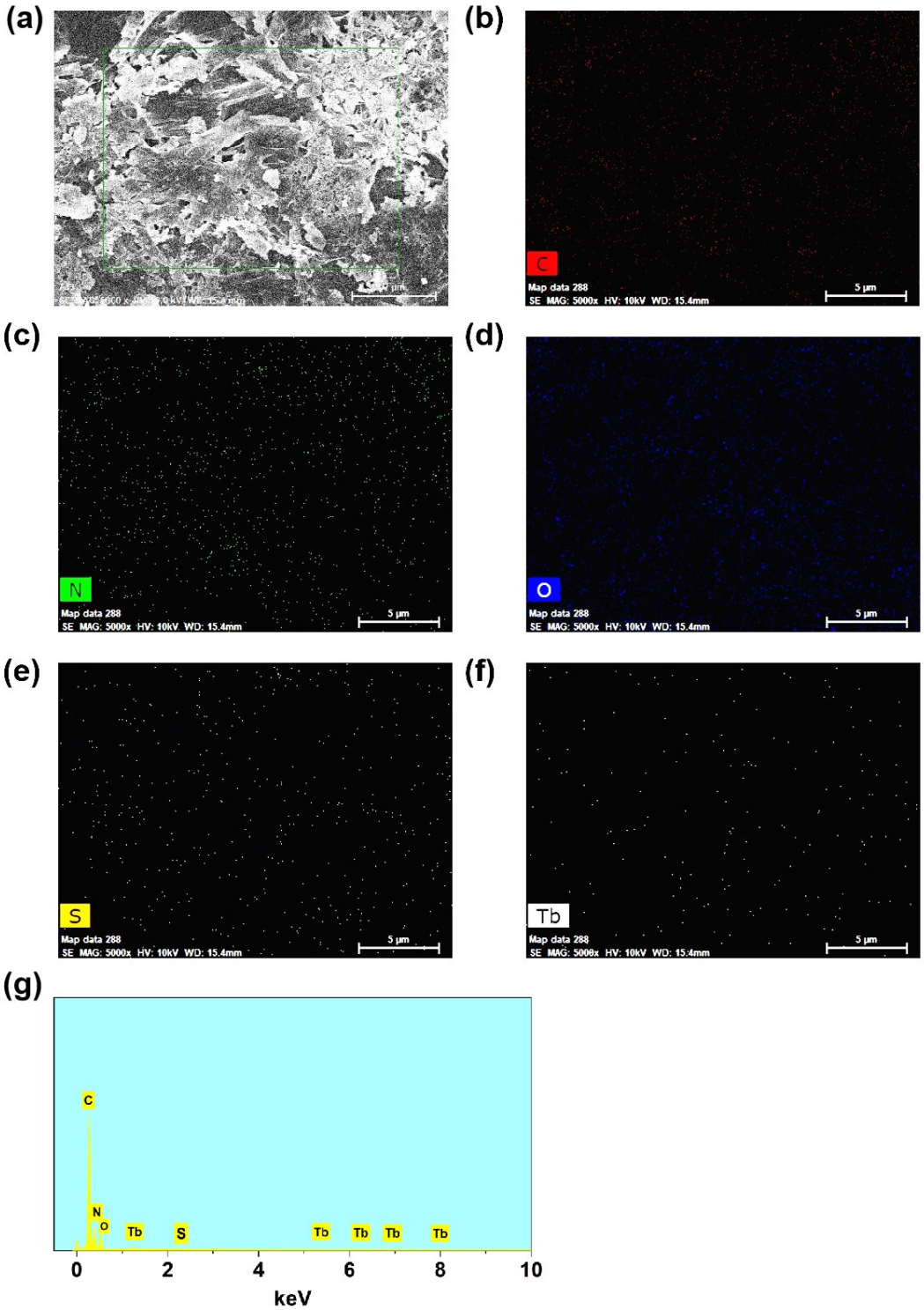

Fig. S10. (a) SEM image of 1-SO_2. (b–f) EDX mapping images of C, N, O and Tb elements in 1-SO_2. (g) The element content of C (45.71%), N (35.97%), O (16.36%), S (0.32%) and Tb (1.64%) elements in EDX energy spectrum of 1-SO_2.

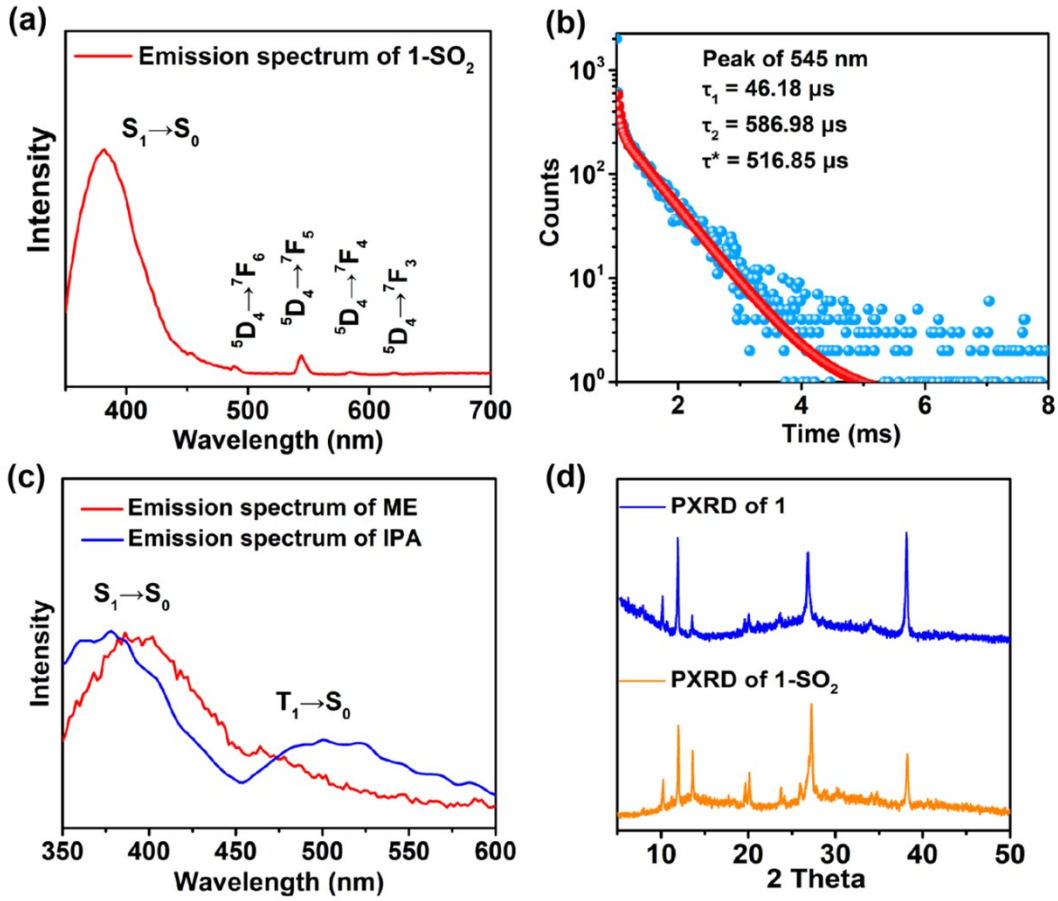

Fig. S11. (a) Emission spectrum of 1-SO_2 (C_{SO2} = 10^{-2} M). (b) Decay lifetime of 545 nm emission peak of **1** (λ_{ex} = 290 nm). (c) Emission spectra of ME and IPA powders. (d) PXRD patterns of **1** and 1-SO_2.

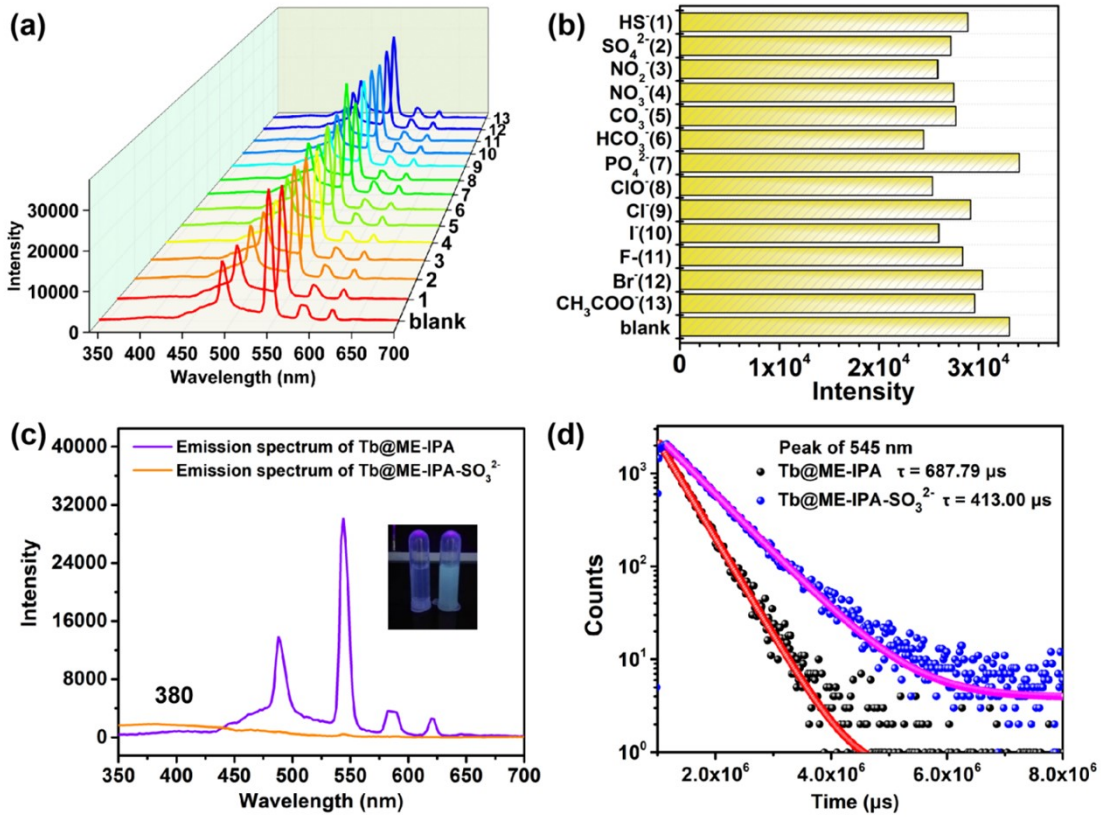

Fig. S12. (a) Emission spectra of Tb@ME-IPA in various anion solution (C = 10^{-2} M) (λ_{ex} = 290 nm). (b) Emission intensity of 545nm peak in various anion solution (C = 10^{-2} M). (c) Emission spectra of Tb@ME-IPA and Tb@ME-IPA-SO_3^{2-} (C = 10^{-2} M) (λ_{ex} = 290 nm). (d) Decay lifetimes of 545 nm emission peak for Tb@ME-IPA and Tb@ME-IPA-SO_3^{2-} (C = 10^{-2} M) (λ_{ex} = 290 nm).

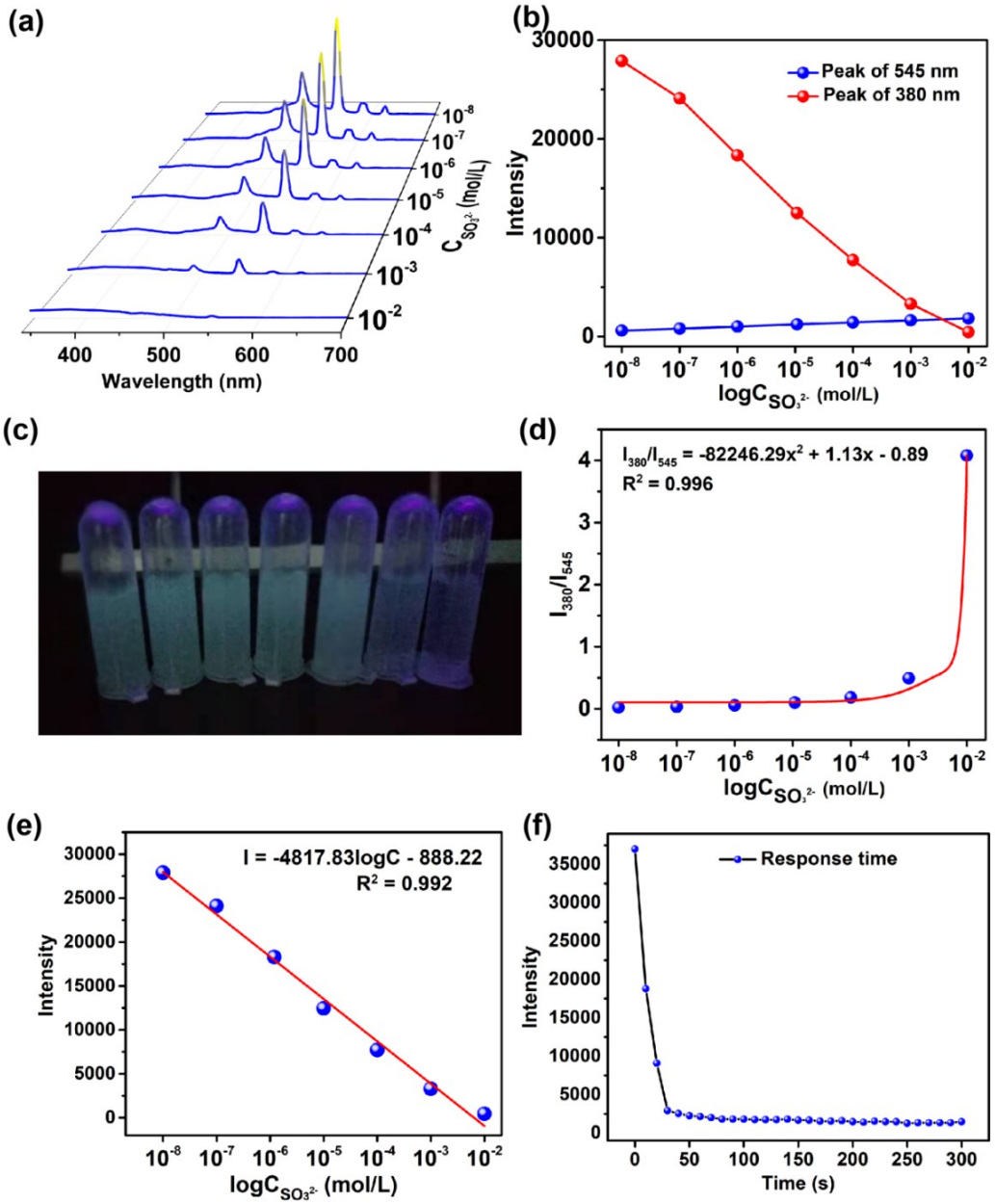

Fig. S13. (a) Emission spectra of Tb@ME-IPA in various SO_3^{2-} solutions with a successive concentration (C = 10^{-8}-10^{-2} M) (λ_{ex} = 290 nm). (b) Dependence of emission intensity of 545 and 380 nm peaks on SO_3^{2-} concentration. (c) Emitting pictures of Tb@ME-IPA in various SO_3^{2-} solutions with a successive concentration (C = 10^{-8}-10^{-2} M) (λ_{ex} = 290 nm). (d) Dependence of emission intensity ratio of 380 and 545 nm peaks on SO_3^{2-} concentration (C = 10^{-8}-10^{-2} M) (e) Calibration curves of Tb@ME-IPA toward SO_3^{2-} in the concentration range of 10^{-8}-10^{-2} M. (f) Response time of Tb@ME-IPA toward SO_3^{2-}.

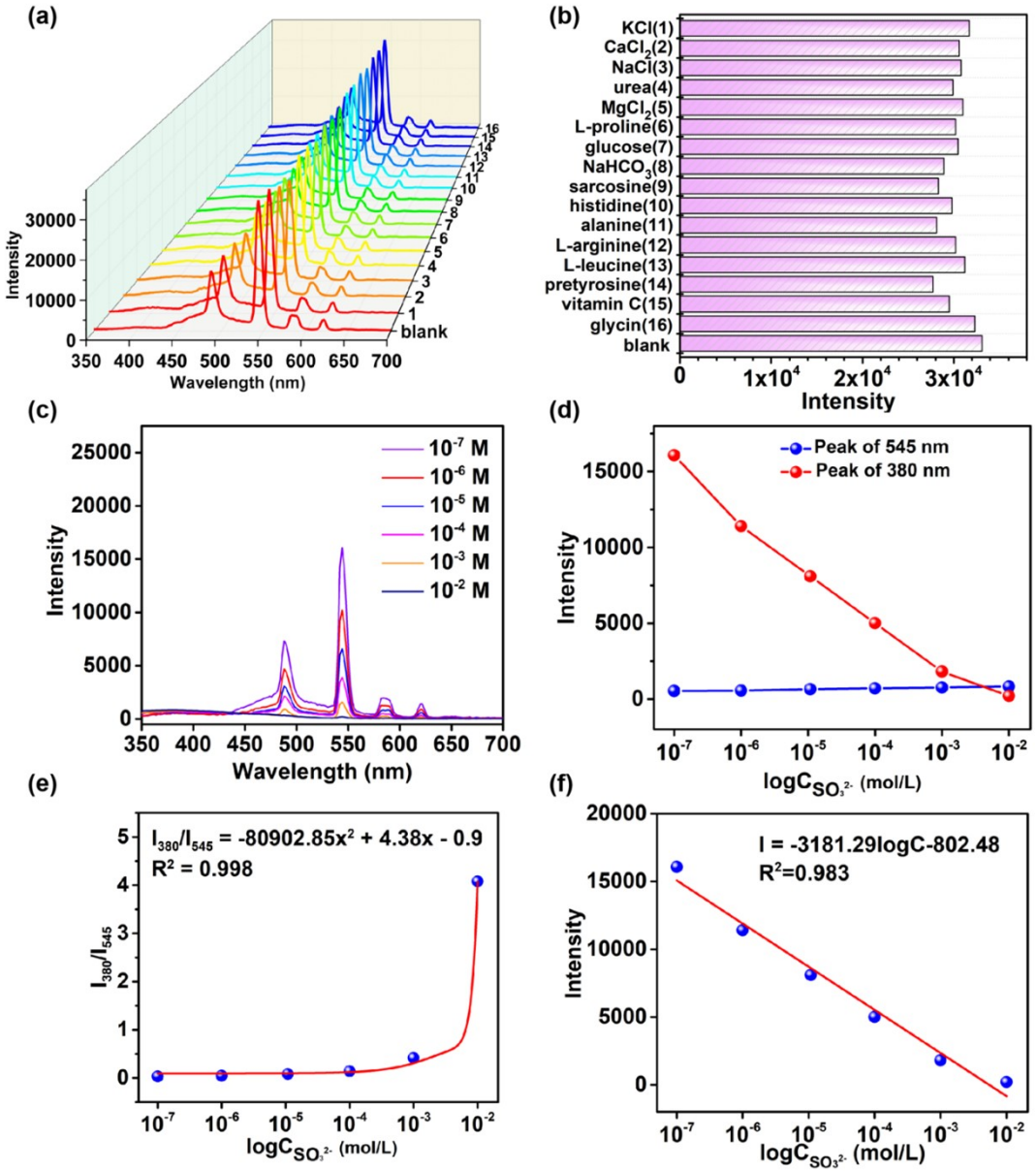

Fig. S14. (a) Emission spectra of Tb@ME-IPA in various serum components (C = 10^{-2} M) (λ_{ex} = 290 nm). (b) Histogram of 545 nm emission peak of Tb@ME-IPA in various serum components (C = 10^{-2} M). (c) Emission spectra of Tb@ME-IPA in serum system in various SO_3^{2-} solutions with a successive concentration (C = 10^{-8}–10^{-2} M) (λ_{ex} = 290 nm). (d) Dependence of emission intensity of 545 and 380 nm peaks on SO_3^{2-} concentration. (e) Dependence of emission intensity ratio of 380 and 545 nm peaks on SO_3^{2-} concentration (10^{-7}–10^{-2} M). (f) Calibration curves of Tb@ME-IPA toward SO_3^{2-} in the concentration range of 10^{-7}–10^{-2} M.

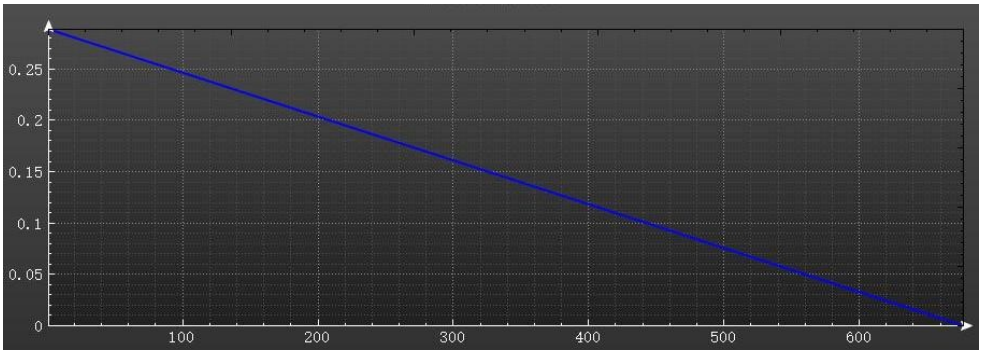

Fig. S15. Network training curve of the BPNN.

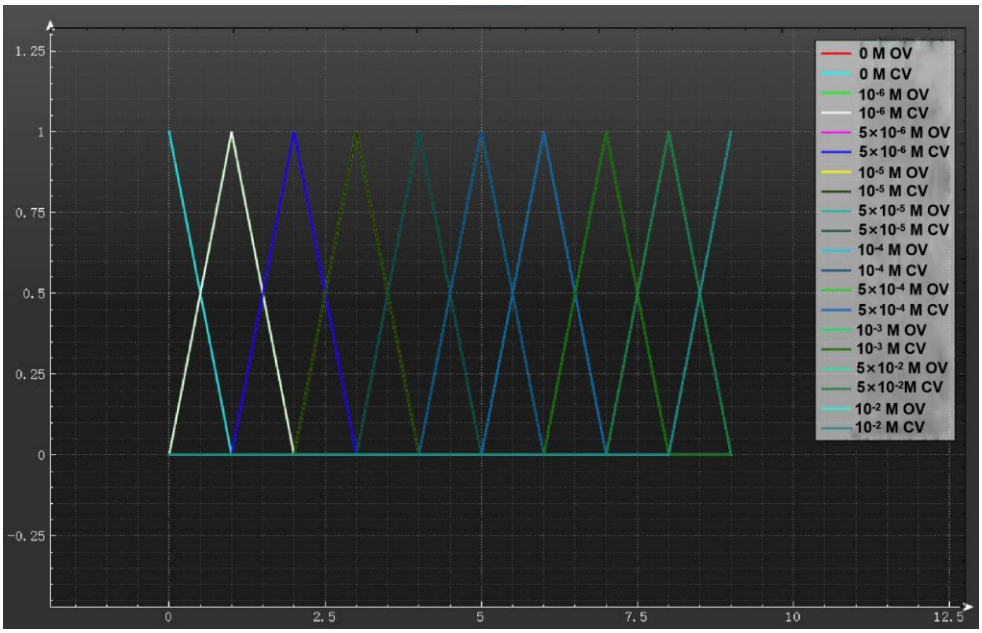

Fig. S16. Deviation curve of the BPNN (OV: original value; CV: calculated value).

In Fig. S16, there are two type of curves respectively representing original value (OV) and calculated value (CV). All curves of OV are overlapped well with the curves of CV, which indicating the low deviation between original and calculated values of output information. Therefore, all curves of OV can not be seen and all curves of CV can only be seen.

Table S1. The reaction equations for preparation of various gases.

NO.	Gas	Reaction equation
1	N_2	$NH_4Cl + NaNO_2 = NaCl + 2H_2O + N_2\uparrow$
2	O_2	$H_2O_2 = 2\ H_2O + O_2\uparrow$ (MnO_2 as catalyzer)
3	CO_2	$Na_2CO_3 + H_2SO_4$ (conc.) $= 2Na_2SO_4 + CO_2\uparrow + H_2O$
4	SO_2	$Na_2SO_3 + H_2SO_4$ (conc.) $= Na_2SO_4 + H_2O + SO_2\uparrow$
5	H_2S	$Na_2S + H_2SO_4$ (conc.) $= Na_2SO_4 + H_2S\uparrow$
6	CO	$HCOOH = CO\uparrow + H_2O$ (H_2SO_4 as catalyzer)
7	NO	$3Na_2SO_3 + 2HNO_3$(dil.) $= 3Na_2SO_4 + 2NO\uparrow + H_2O$
8	NO_2	$2KI + 4HNO_3$(conc.) $= I_2 + 2NO_2\uparrow + 2KNO_3 + 2H_2O$
9	H_2	$Zn + H_2SO_4 = ZnSO_4 + H_2\uparrow$
10	CH_4	$CH_3COONa + NaOH = \triangle = Na_2CO_3 + CH_4\uparrow$ (CaO as catalyzer)
11	NH_3	volatilization of ammonia
12	C_7H_8	volatilization of toluene
13	CH_3OH	volatilization of methanol
14	C_2H_5OH	volatilization of ethanol
15	CH_3COCH_3	volatilization of acetone

Table S2. Element contents of C, N, O, Tb in EDX energy spectrum **1** and C, N, O, S, Tb in EDX energy spectrum 1-SO_2.

1		1-SO_2	
Elements	W_t%	Elements	W_t%
C	53.52	C	45.71
N	36.52	N	33.97
O	8.39	O	16.36
Tb	1.57	S	2.64
		Tb	1.32

Table S3. Summary of decay lifetime of **1**, 1-SO_2, Tb@ME-IPA, and Tb@ME-IPA-SO_3^{2-}.

Sample	λ_{ex} (nm)	λ_{em} (nm)	τ_1 (μs)	A_1	Percentage (%)	τ_2 (μs)	A_2	Percentage (%)	τ^*	χ^2
1	290	545	597.43	1510.98	61.42	1076.77	526.56	38.58	790.24	1.457
1-SO_2	290	545	46.18	496.88	12.97	586.98	262.36	87.03	516.85	1.070
Tb@ME-IPA	290	545	687.79	2019.57	100.00	-	-	-	-	1.390
Tb@ME-IPA-SO_3^{2-}	290	545	413.00	2181.39	100.00	-	-	-	-	1.181

Table S4. Summary of emission transitions and experimental energy gaps of ME-IPA and Tb^{3+} ions.

	Transitions	Wavelength (nm)	Energy gap (eV)
ME-IPA	$S_1 \rightarrow S_0$	359	3.45
	$T_1 \rightarrow S_0$	486	2.55
Tb^{3+}	$^5D_4 \rightarrow {}^7F_K$	488	2.54
	$^5D_4 \rightarrow {}^7F_K$	545	2.28
	$^5D_4 \rightarrow {}^7F_K$	583	2.13
	$^5D_4 \rightarrow {}^7F_K$	621	2.00

Table S5. Summary of R.G.B. of emitting color of **1** exposed in various SO_2 concentration (10^{-6}-10^{-2} M).

Concentration	10^{-6}	10^{-5}	10^{-4}	10^{-3}	10^{-2}
Color	PaleGreen1	DarkSeaGreen3	lavender	SlateBlue3	SlateBlue4
Picture					
R.G.B	154 255 154	155 205 155	230 230 250	105 89 205	71 60 139
Concentration	5×10^{-6}	5×10^{-5}	5×10^{-4}	5×10^{-3}	0

Color	SeaGreen1	DarkSeaGreen 1	MediumPurple 1	Blue4	PaleGreen
Picture					
R.G.B	84 255 159	193 255 193	171 130 255	0 0 139	152 251 152

Table S6. Summary of input and output information during the training of BPNN for SO_2 detection.

Picture	Input (R.G.B value)			Output [Concentration of SO_2 (M)]									
	R	G	B	0	10^{-6}	5×10^{-6}	10^{-5}	5×10^{-6}	10^{-4}	5×10^{-6}	10^{-3}	5×10^{-6}	10^{-2}
	152	251	152	1	0	0	0	0	0	0	0	0	0
	154	255	154	0	1	0	0	0	0	0	0	0	0
	84	255	159	0	0	1	0	0	0	0	0	0	0
	155	205	155	0	0	0	1	0	0	0	0	0	0
	193	255	193	0	0	0	0	1	0	0	0	0	0
	230	230	250	0	0	0	0	0	1	0	0	0	0
	171	130	255	0	0	0	0	0	0	1	0	0	0
	105	89	205	0	0	0	0	0	0	0	1	0	0
	0	0	139	0	0	0	0	0	0	0	0	1	0
	71	60	139	0	0	0	0	0	0	0	0	0	1

In Table S6, all data is used to training the BPNN. The R.G.B values of every color as input information are inputted in the input column of the BPNN. Various “0” and “1” inputted into the output column of the BPNN, in which “0” represents the false SO_2 concentration, and “1” represents the correct SO_2 concentration. All data is used to train the BPNN.

Table S7. Network structure information.

Network structure information		
Input layer	3 neurons	1 Paranoid
Hidden layer 1	5 neurons	1 Paranoid
Output layer	10neurons	
Network type	FANN_NETTYPE_LAYER	
Training function	FANN_TRAIN_RPROP	
Error function	FANN_ERRORFUNC_LINEAR	
Termination function	FANN_STOPFUNC_MSE	
Hidden layer excitation function	FANN_SIGMOID_SYMMETRIC	
Output layer excitation function	FANN_SIGMOID_SYMMETRIC	

Network weight value

Arrangement	Wire number	Output point (n)	Input point (m)	Weight value (*W*)
1	0	0	4	-2.17058
	1	1	4	2.57524
	2	2	4	0.698852
	3	3	4	-1.39816
	4	0	5	-43.6209
	5	1	5	-450.595
	6	2	5	0.0045888
	7	3	5	-1448
	8	0	6	-0.119756
	9	1	6	0.562446
	10	2	6	2.00202
	11	3	6	-2.59579
	12	0	7	6.57045
	13	1	7	-1.05856
	14	2	7	5.28074
	15	3	7	2.98667
	16	0	8	-2.73271
	17	1	8	0.0701685
	18	2	8	2.79813
	19	3	8	2.20223
	20	4	10	31.5016
	21	5	10	10.9008
	22	6	10	2.08634
2	23	7	10	-140.654
	24	8	10	-231.037
	25	9	10	-20.8311
	26	4	11	372.743

27	5	11	1.01869
28	6	11	-0.166004
29	7	11	106.199
30	8	11	-170.102
31	9	11	-6.412
32	4	12	1500
33	5	12	1500
34	6	12	1500
35	7	12	189.882
36	8	12	1500
37	9	12	1500
38	4	13	-155.524
39	5	13	4.05623
40	6	13	0.180367
41	7	13	40.7606
42	8	13	-155.069
43	9	13	-81.8848
44	4	14	278.475
45	5	14	25.7603
46	6	14	5.32007
47	7	14	144.396
48	8	14	-18.4874
49	9	14	-12.1015
50	4	15	1500
51	5	15	1500
52	6	15	1500
53	7	15	1204.98
54	8	15	940.559
55	9	15	1203.07
56	4	16	-160.791
57	5	16	39.0143
58	6	16	105.367
59	7	16	1.56348
60	8	16	15.5595
61	9	16	-24.122
62	4	17	-6.50918
63	5	17	9.84273
64	6	17	-72.4171
65	7	17	17.6102
66	8	17	29.5826
67	9	17	-87.4224
68	4	18	-26.4926
69	5	18	136.401
70	6	18	0.223098

	71	7	18	-44.1377
	72	8	18	158.281
	73	9	18	-23.7568
	74	4	19	-44.9046
	75	5	19	25.2329
	76	6	19	0.697594
	77	7	19	-64.528
	78	8	19	-95.4034
	79	9	19	-18.2412

Input / output column coefficients for manual calculation

Listing	Minimum	Maximum
R	0	242.105
G	0	268.421
B	132.05	268.421
0 M	0	1
0.000001 M	0	1
0.000005 M	0	1
0.00001 M	0	1
0.00005 M	0	1
0.0001 M	0	1
0.0005 M	0	1
0.001 M	0	1
0.005 M	0	1
0.01 M	0	1

Deviation statistics: mean variance

Listing	All rows	Calculation line	Test line
0 M	6.6085e-10	6.6085e-10	0
0.000001 M	2.8365e-10	2.8365e-10	0
0.000005 M	2.5e-14	2.5e-14	0
0.00001 M	0	0	0
0.00005 M	0	0	0
0.0001 M	0	0	0
0.0005 M	0	0	0
0.001 M	6.825e-12	6.825e-12	0
0.005 M	0	0	0
0.01 M	0	0	0

Table S8. The summary of mean square error (MSE), original value (OV), calculated value (CV), variance (Var.)

1	Input item			0 M (MSE = 6.6085e-10)			0.000001 M (MSE = 2.8365e-10)			0.000005 M (MSE = 2.5e-14)			0.00001 M (MSE = 0)		
2	R	G	B	OV.	CV.	Var.	OV.	CV.	Var.	OV.	CV.	Var.	OV.	CV.	Var.
3	152	251	152	**1**	**0.999934**	4.356e-09	0	3.25e-05	1.05625e-09	0	0	0	0	0	0
4	154	255	154	0	4.65e-05	2.16225e-09	**1**	**0.999958**	1.764e-09	0	0	0	0	0	0
5	84	255	159	0	0	0	0	2e-06	4e-12	**1**	**1**	0	0	0	0
6	155	205	155	0	0	0	0	0	0	0	0	0	**1**	**1**	0
7	193	255	193	0	0	0	0	3.5e-06	1.225e-11	0	0	0	0	0	0
8	230	230	250	0	0	0	0	0	0	0	5e-07	2.5e-13	0	0	0
9	171	130	255	0	0	0	0	0	0	0	0	0	0	0	0
10	105	89	205	0	0	0	0	0	0	0	0	0	0	0	0
11	0	0	139	0	0	0	0	0	0	0	0	0	0	0	0
12	71	60	139	0	9.5e-06	9.025e-11	0	0	0	0	0	0	0	0	0

1	0.00005 M(MSE = 0)			0.0001 M(MSE = 0)			0.0005 M(MSE = 0)			0.001 M(MSE = 6.825e-12)			0.005 M(MSE = 0)			0.01 M(MSE = 0)		
2	OV.	CV.	Var.	OV.	CV.	Var.	OV.	CV.	Var.	OV.	CV.	Var.	OV.	CV.	Var.	OV.	CV.	Var.
3	0	0	0	0	0	0	0	0	0	0	0	0	0	0	0	0	0	0
4	0	0	0	0	0	0	0	0	0	0	0	0	0	0	0	0	0	0
5	0	0	0	0	0	0	0	0	0	0	0	0	0	0	0	0	0	0
6	0	0	0	0	0	0	0	0	0	0	0	0	0	0	0	0	0	0
7	**1**	**1**	0	0	0	0	0	0	0	0	1.5e-06	2.25e-12	0	0	0	0	0	0
8	0	0	0	**1**	**1**	0	0	0	0	0	0	0	0	0	0	0	0	0
9	0	0	0	0	0	0	**1**	**1**	0	0	4e-06	1.6e-11	0	0	0	0	0	0
10	0	0	0	0	0	0	0	0	0	**1**	**0.999993**	4.9e-11	0	0	0	0	0	0
11	0	0	0	0	0	0	0	0	0	0	1e-06	1e-12	**1**	**1**	0	0	0	0
12	0	0	0	0	0	0	0	0	0	0	0	0	0	0	0	**1**	**1**	0

In Table S8, all data is utilized to test the BPNN. The R.G.B values of every color as input information are inputted in the input column of the BPNN. Through the BPNN calculation, various values (0-1) can be outputted, in which the values close to "0" represents the false SO_2 concentration, the values close to "1" represents the correct SO_2 concentration. By comparing the OV with CV, the variance can be obtained, which suggests that the BPNN has a good accuracy for detecting SO_2 concentration.

Table S9. The summary of input and output information in real batch calculation during the test of BPNN.

Input data			Output data									
R	G	B	0 M	0.000001 M	0.000005 M	0.00001 M	0.00005 M	0.0001 M	0.0005 M	0.001 M	0.005 M	0.01 M
152	251	152	**0.999934**	3.25864e-05	0	0	0	0	0	1.44329e-15	0	1.50328e-09
154	255	154	4.66943e-05	**0.999958**	0	0	0	0	0	1.16573e-14	0	3.747e-14
84	255	159	5.66547e-13	1.76799e-06	**1**	0	0	0	0	1.53211e-14	5.55112e-17	0
155	205	155	0	0	0	**1**	0	0	0	2.66377e-11	0	1.87311e-12
193	255	193	0	3.37203e-06	0	5.55112e-17	**1**	0	0	1.71061e-06	0	0
230	230	250	0	0	5.81046e-07	0	5.55112e-17	**1**	2.20176e-08	3.34388e-12	0	0
171	130	255	0	0	0	0	0	4.35348e-10	**1**	3.93021e-06	5.55112e-17	0
105	89	205	0	0	0	0	0	0	4.24601e-09	**0.999993**	0	0
0	0	139	0	0	0	0	0	0	9.54616e-10	1.14786e-06	**1**	8.37655e-10
71	60	139	9.49636e-06	0	0	0	0	0	1.89536e-11	2.9306e-12	1.11022e-16	**1**

In Table S9, all data is utilized to test the BPNN. The R.G.B values of every color as input information are inputted in the input column of the BPNN. Through the BPNN calculation, various values (0-1) can be acquired, in which the values close to "0" represents the false SO_2 concentration, and the values close to 1 represents the correct SO_2 concentration.

Table S10. The matlab code of this BPNN.

Matlab code

```
function [fO0, fO1, fO2, fO3, fO4, fO5, fO6, fO7, fO8, fO9] = MPredict(fI0, fI1, fI2)
    fI0 = (fI0 - (0 + 242.1052631578947398 ) / 2.0) /(242.1052631578947398 - (0 + 242.1052631578947398 ) / 2.0);
    fI1 = (fI1 - (0 + 268.4210526315789593 ) / 2.0) /(268.4210526315789593 - (0 + 268.4210526315789593 ) / 2.0);
    fI2 = (fI2 - (132.0499999999999829 + 268.4210526315789593 ) / 2.0) /(268.4210526315789593 - (132.0499999999999829 + 268.4210526315789593 ) /
2.0);
    fWei0 = -2.17058;
    fWei1 = 2.57524;
    fWei2 = 0.698852;
    fWei3 = -1.39816;
    fWei4 = -43.6209;
    fWei5 = -450.595;
    fWei6 = 0.0045888;
    fWei7 = -1448;
    fWei8 = -0.119756;
    fWei9 = 0.562446;
    fWei10 = 2.00202;
    fWei11 = -2.59579;
    fWei12 = 6.57045;
    fWei13 = -1.05856;
    fWei14 = 5.28074;
    fWei15 = 2.98667;
    fWei16 = -2.73271;
```

```
fWei17 = 0.0701685;
fWei18 = 2.79813;
fWei19 = 2.20223;
fWei20 = 31.5016;
fWei21 = 10.9008;
fWei22 = 2.08634;
fWei23 = -140.654;
fWei24 = -231.037;
fWei25 = -20.8311;
fWei26 = 372.743;
fWei27 = 1.01869;
fWei28 = -0.166004;
fWei29 = 106.199;
fWei30 = -170.102;
fWei31 = -6.412;
fWei32 = 1500;
fWei33 = 1500;
fWei34 = 1500;
fWei35 = 189.882;
fWei36 = 1500;
fWei37 = 1500;
fWei38 = -155.524;
fWei39 = 4.05623;
fWei40 = 0.180367;
fWei41 = 40.7606;
fWei42 = -155.069;
fWei43 = -81.8848;
fWei44 = 278.475;
fWei45 = 25.7603;
fWei46 = 5.32007;
fWei47 = 144.396;
fWei48 = -18.4874;
fWei49 = -12.1015;
fWei50 = 1500;
fWei51 = 1500;
fWei52 = 1500;
fWei53 = 1204.98;
fWei54 = 940.559;
fWei55 = 1203.07;
fWei56 = -160.791;
fWei57 = 39.0143;
fWei58 = 105.367;
fWei59 = 1.56348;
fWei60 = 15.5595;
fWei61 = -24.122;
fWei62 = -6.50918;
fWei63 = 9.84273;
fWei64 = -72.4171;
fWei65 = 17.6102;
fWei66 = 29.5826;
fWei67 = -87.4224;
fWei68 = -26.4926;
fWei69 = 136.401;
fWei70 = 0.223098;
fWei71 = -44.1377;
fWei72 = 158.281;
fWei73 = -23.7568;
```

```
fWei74 = -44.9046;
fWei75 = 25.2329;
fWei76 = 0.697594;
fWei77 = -64.528;
fWei78 = -95.4034;
fWei79 = -18.2412;
f0 = fI0;
f1 = fI1;
f2 = fI2;
f3 = 1.0;
f4 = 0.0;
f5 = 0.0;
f6 = 0.0;
f7 = 0.0;
f8 = 0.0;
f4 = f4 + f0 * fWei0;
f4 = f4 + f1 * fWei1;
f4 = f4 + f2 * fWei2;
f4 = f4 + f3 * fWei3;
f4 = f4 * 0.5;
f4 = (2.0 / (1.0 + exp(-2.0 * f4))- 1.0);
f5 = f5 + f0 * fWei4;
f5 = f5 + f1 * fWei5;
f5 = f5 + f2 * fWei6;
f5 = f5 + f3 * fWei7;
f5 = f5 * 0.5;
f5 = (2.0 / (1.0 + exp(-2.0 * f5))- 1.0);
f6 = f6 + f0 * fWei8;
f6 = f6 + f1 * fWei9;
f6 = f6 + f2 * fWei10;
f6 = f6 + f3 * fWei11;
f6 = f6 * 0.5;
f6 = (2.0 / (1.0 + exp(-2.0 * f6))- 1.0);
f7 = f7 + f0 * fWei12;
f7 = f7 + f1 * fWei13;
f7 = f7 + f2 * fWei14;
f7 = f7 + f3 * fWei15;
f7 = f7 * 0.5;
f7 = (2.0 / (1.0 + exp(-2.0 * f7))- 1.0);
f8 = f8 + f0 * fWei16;
f8 = f8 + f1 * fWei17;
f8 = f8 + f2 * fWei18;
f8 = f8 + f3 * fWei19;
f8 = f8 * 0.5;
f8 = (2.0 / (1.0 + exp(-2.0 * f8))- 1.0);
f9 = 1.0;
f10 = 0.0;
f11 = 0.0;
f12 = 0.0;
f13 = 0.0;
f14 = 0.0;
f15 = 0.0;
f16 = 0.0;
f17 = 0.0;
f18 = 0.0;
f19 = 0.0;
f10 = f10 + f4 * fWei20;
```

```
f10 = f10 + f5 * fWei21;
f10 = f10 + f6 * fWei22;
f10 = f10 + f7 * fWei23;
f10 = f10 + f8 * fWei24;
f10 = f10 + f9 * fWei25;
f10 = f10 * 0.5;
f10 = (2.0 / (1.0 + exp(-2.0 * f10))- 1.0);
f11 = f11 + f4 * fWei26;
f11 = f11 + f5 * fWei27;
f11 = f11 + f6 * fWei28;
f11 = f11 + f7 * fWei29;
f11 = f11 + f8 * fWei30;
f11 = f11 + f9 * fWei31;
f11 = f11 * 0.5;
f11 = (2.0 / (1.0 + exp(-2.0 * f11))- 1.0);
f12 = f12 + f4 * fWei32;
f12 = f12 + f5 * fWei33;
f12 = f12 + f6 * fWei34;
f12 = f12 + f7 * fWei35;
f12 = f12 + f8 * fWei36;
f12 = f12 + f9 * fWei37;
f12 = f12 * 0.5;
f12 = (2.0 / (1.0 + exp(-2.0 * f12))- 1.0);
f13 = f13 + f4 * fWei38;
f13 = f13 + f5 * fWei39;
f13 = f13 + f6 * fWei40;
f13 = f13 + f7 * fWei41;
f13 = f13 + f8 * fWei42;
f13 = f13 + f9 * fWei43;
f13 = f13 * 0.5;
f13 = (2.0 / (1.0 + exp(-2.0 * f13))- 1.0);
f14 = f14 + f4 * fWei44;
f14 = f14 + f5 * fWei45;
f14 = f14 + f6 * fWei46;
f14 = f14 + f7 * fWei47;
f14 = f14 + f8 * fWei48;
f14 = f14 + f9 * fWei49;
f14 = f14 * 0.5;
f14 = (2.0 / (1.0 + exp(-2.0 * f14))- 1.0);
f15 = f15 + f4 * fWei50;
f15 = f15 + f5 * fWei51;
f15 = f15 + f6 * fWei52;
f15 = f15 + f7 * fWei53;
f15 = f15 + f8 * fWei54;
f15 = f15 + f9 * fWei55;
f15 = f15 * 0.5;
f15 = (2.0 / (1.0 + exp(-2.0 * f15))- 1.0);
f16 = f16 + f4 * fWei56;
f16 = f16 + f5 * fWei57;
f16 = f16 + f6 * fWei58;
f16 = f16 + f7 * fWei59;
f16 = f16 + f8 * fWei60;
f16 = f16 + f9 * fWei61;
f16 = f16 * 0.5;
f16 = (2.0 / (1.0 + exp(-2.0 * f16))- 1.0);
f17 = f17 + f4 * fWei62;
f17 = f17 + f5 * fWei63;
```

```
f17 = f17 + f6 * fWei64;
f17 = f17 + f7 * fWei65;
f17 = f17 + f8 * fWei66;
f17 = f17 + f9 * fWei67;
f17 = f17 * 0.5;
f17 = (2.0 / (1.0 + exp(-2.0 * f17))- 1.0);
f18 = f18 + f4 * fWei68;
f18 = f18 + f5 * fWei69;
f18 = f18 + f6 * fWei70;
f18 = f18 + f7 * fWei71;
f18 = f18 + f8 * fWei72;
f18 = f18 + f9 * fWei73;
f18 = f18 * 0.5;
f18 = (2.0 / (1.0 + exp(-2.0 * f18))- 1.0);
f19 = f19 + f4 * fWei74;
f19 = f19 + f5 * fWei75;
f19 = f19 + f6 * fWei76;
f19 = f19 + f7 * fWei77;
f19 = f19 + f8 * fWei78;
f19 = f19 + f9 * fWei79;
f19 = f19 * 0.5;
f19 = (2.0 / (1.0 + exp(-2.0 * f19))- 1.0);
fO0 = f10;
fO1 = f11;
fO2 = f12;
fO3 = f13;
fO4 = f14;
fO5 = f15;
fO6 = f16;
fO7 = f17;
fO8 = f18;
fO9 = f19;
fO0 = fO0 * (1 - (0 + 1 ) / 2.0) + (0 + 1) / 2.0;
fO1 = fO1 * (1 - (0 + 1 ) / 2.0) + (0 + 1) / 2.0;
fO2 = fO2 * (1 - (0 + 1 ) / 2.0) + (0 + 1) / 2.0;
fO3 = fO3 * (1 - (0 + 1 ) / 2.0) + (0 + 1) / 2.0;
fO4 = fO4 * (1 - (0 + 1 ) / 2.0) + (0 + 1) / 2.0;
fO5 = fO5 * (1 - (0 + 1 ) / 2.0) + (0 + 1) / 2.0;
fO6 = fO6 * (1 - (0 + 1 ) / 2.0) + (0 + 1) / 2.0;
fO7 = fO7 * (1 - (0 + 1 ) / 2.0) + (0 + 1) / 2.0;
fO8 = fO8 * (1 - (0 + 1 ) / 2.0) + (0 + 1) / 2.0;
fO9 = fO9 * (1 - (0 + 1 ) / 2.0) + (0 + 1) / 2.0;
```